

# RHEOLOGICAL STUDIES OF ORGANICALLY-MODIFIED CLAY DISPERSIONS IN STEADY AND TRANSIENT SHEAR FLOWS

**Jin Li**

Department of Chemical Engineering  
University of Virginia  
Charlottesville, VA 22904-4741, U.S.A.  
[lijin@virginia.edu](mailto:lijin@virginia.edu)

**James P. Oberhauser**

Department of Chemical Engineering  
University of Virginia  
Charlottesville, VA 22904-4741, U.S.A.  
[oberhauser@virginia.edu](mailto:oberhauser@virginia.edu)

## ABSTRACT

This work examines the rheological behavior of exfoliated dispersions of organically modified montmorillonite clay in *p*-xylene. The clay loadings in these dispersions range from 0.5 wt% to 4 wt%, and they have been studied under oscillatory shear, steady shear, and double-step shear stress flows. The dispersions exhibit a storage modulus plateau whose magnitude varies over three orders of magnitude, depending upon clay loading, which is consistent with a solid-like, percolated clay network. All samples also exhibit a yield stress whose magnitude also increases with clay loading. Like many yield stress fluids, these dispersions also show a shear stress vs. shear rate hysteresis, suggesting that once the clay network has been disrupted, flow can prevent it from reforming even at shear stresses somewhat less than the yield stress. Within the hysteresis regime, the viscosity shows time-periodic behavior, raising the possibility that the balance between flow and network reformation is unstable at those shear stresses. Finally, preliminary data demonstrate that the time scale for network reformation depends strongly upon the initial shear stress. We intend to use these results to further clarify the physics of the percolated clay network.

## INTRODUCTION

Solid, inorganic filler material is frequently added to polymer melts to enhance mechanical, dielectric, electric, or thermal properties. Glass and carbon fiber-reinforced composites are common examples. However, fiber-reinforced composites are prone to reduced ductility, poor moldability, and surface roughness, and, because fibers are microscale in dimension, the filler composition is often on the order of 30 vol% in order to provide the necessary property enhancement.

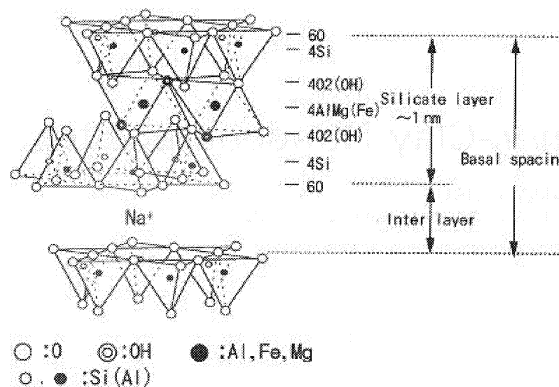


**Figure 1.** Schematic representation of a natural Na<sup>+</sup> montmorillonite clay [excerpted from Kato and Usuki (2000)]

More recently, polymer-clay nanocomposites (PCNs) have attracted strong research and commercial interest due to profound improvements in material properties (e.g., increased tensile strength, modulus, and heat resistance and reduced gas permeability) with only modest clay loading. One such clay is montmorillonite, which consists of layered planar silicates 1 nm thick and lateral dimensions of 300 – 1,000 nm, separated by a Van der Waals interlayer (see Figure 1). Through the addition of surfactant, the interlayer may be rendered organophilic via a cation exchange process with a surfactant. Depending upon the choice of surfactant, the resulting organically modified montmorillonite clay is compatible with many organic solvents and hydrophobic polymers, which is essential for numerous industrial applications.

Importantly, even at a few vol%, the number of nanometric clay platelets and amount of clay surface area is

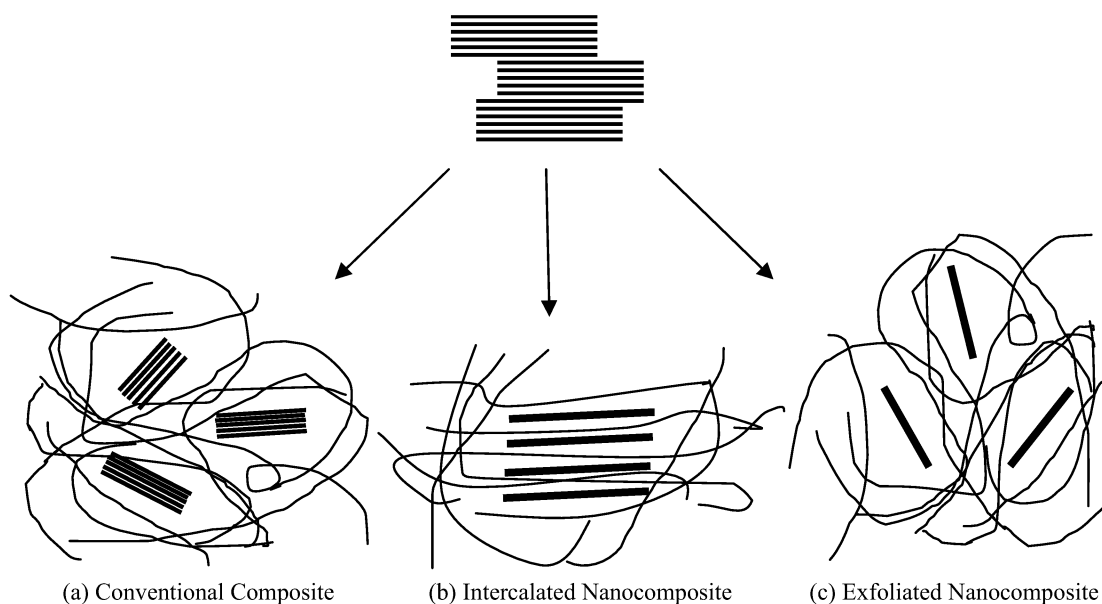


**Figure 2.** Schematic representation of the three possible structures obtained upon adding montmorillonite clay to a polymer matrix.

enormous, maximizing the interfacial contact of the clay and polymer molecules, a necessity for the clay species to act as a load bearing filler material. Pioneering research at Toyota Central Research Laboratories demonstrated significant material property improvements for systems with as little as 2 vol% montmorillonite clay in a nylon-6 matrix [Kojima *et al.* (1993)].

Figure 2 shows the three possible structures formed when montmorillonite clay is added to a polymer matrix. If the two species have unfavorable surface chemistry, clay platelets form micron scale aggregates akin to conventional composite materials. As the surface chemistry becomes more favorable, intercalated and exfoliated nanocomposite materials are possible. Much of the aforementioned material property enhancements rely upon the successful exfoliation of the clay platelets. This issue has been the focus of a number of studies that have applied a battery of experimental techniques, including small-angle neutron scattering (SANS), x-ray diffraction (XRD), small- and wide-angle x-ray scattering (SAXS and WAXS), atomic force microscopy (AFM), and transmission electron microscopy (TEM), to conclude that complete exfoliation is difficult to achieve [Hanley *et al.* (2003), Ho *et al.* (2001), Ho and Glinka (2003), Vaia *et al.* (2003)]. For example, Ho and Glinka (2003) used SANS and WAXS to show that Cloisite® 15A (C15A), a commercial organically modified montmorillonite produced by Southern Clay Products, was fully exfoliated in chloroform and trichloroethylene and formed tactoids of approximately two silicate layers in *p*-xylene. Other solvents, such as tetrahydrofuran, cyclohexane, and acetone, saw C15A precipitate out of solution altogether.

As in fiber-reinforced polymeric materials, it is likely that many of the improved material properties also derive from the microstructure formed by the highly anisotropic clay platelets and the polymer matrix. Since traditional

polymer processing applications (e.g., injection molding, extrusion, blow molding) involve complex flows that strongly affect the microstructure and rheology of polymer melts and suspensions, a detailed understanding of the relationship between the clay microstructure and macroscopic properties in flow is essential to economically and reliably manufacture products from these materials.

Because the thermodynamic phase behavior of polymer-clay nanocomposite systems is quite complex, clay-solvent dispersions offer a simpler model system from which to begin analyzing structure-property relationships and networking properties of dispersed clay. Recently, Zhong and Wang (2003) studied the rheology of dispersions of Cloisite® 20A (which differs from C15A only in the amount of surfactant added) in *p*-xylene at loadings ranging from 1 – 10 wt%. Using cone-and-plate and parallel plate geometries in a controlled stress rheometer, the authors observed steeply increasing modulus and low-stress viscosity with increasing clay loading and yield stresses in the range of 4 – 10<sup>3</sup> Pa, where the yield stress also increases with clay loading. The results strongly suggest that the clay platelets form a gel-like, percolated network that is destroyed at some critical (yield) shear stress.

In the work reported here, we present mechanical rheology data for C15A dispersions in *p*-xylene at loadings ranging from 0.5 – 4.0 wt%, where the samples have been prepared in a fashion consistent with that of Ho and Glinka (2003). Because C15A contains surfactant in 30% excess of the cation exchange capacity of the natural Na<sup>+</sup>-montmorillonite, we have also removed the excess surfactant using a filtration process [Hanley *et al.* (2001)] in order to assess the effect of excess surfactant on rheological properties. These extracted samples will hereafter be referred to as EC15A. All samples were subjected to oscillatory shear flow and steady shear flow in

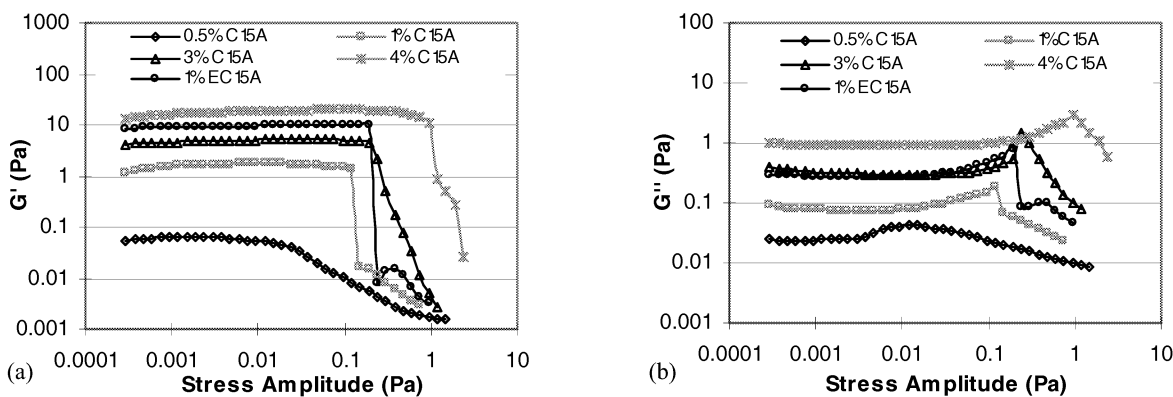


Figure 3. (a) Storage modulus and (b) loss modulus under oscillatory shear at 1 rad/s with varying stress amplitude.

order to characterize their yield behavior and viscosity as a function of clay loading and deformation history.

## EXPERIMENTAL

### Sample Preparation

The solution exfoliation method of Ho and Glinka (2003) was used to prepare solutions of 0.5, 1.0, 2.0, 3.0, and 4.0 wt% montmorillonite clay were made by dissolving as-received Cloisite® 15A (C15A) from Southern Clay Products in *p*-xylene (Sigma-Aldrich). C15A is made from Na<sup>+</sup>-montmorillonite via a cation exchange reaction with a dimethyl dihydrogenated tallow quaternary ammonium chloride surfactant. The tallow group is a mixture of approximately 65% 18 carbon chains, 30% 16 carbon chains, and 5% 14 carbon chains. The cation exchange reaction lowers the surface energy of the montmorillonite, thereby increasing compatibility with organic compounds. *p*-Xylene was selected as a solvent because of its well-documented ability to exfoliate C15A and its relatively high boiling point (138°C), which minimizes solvent evaporation. Each sample was sonicated for one hour and then stored for several days before use. All samples were transparent or translucent prior to use, as expected for an exfoliated clay dispersion and a refractive index matched system.

### Mechanical Rheology

Yield behavior in gel-like systems is best studied in a controlled stress rheometer. Hence, mechanical rheology was performed using a TA Instruments AR2000 controlled stress rheometer at 20°C. Oscillatory shear and steady shear experiments were performed to characterize the response of the fluids to various deformation histories. Depending upon the viscosity of the samples, either single-cup or double-cup concentric cylinder Couette geometries were used to impose shear flow. The Couette geometries are equipped with a solvent trap to minimize the effect of solvent evaporation. From these experiments, one can measure the storage and loss moduli ( $G'$  and  $G''$ ) and viscosity as a function of shear stress (or shear rate). The storage modulus is a measure of elasticity, or the fluid's ability to store energy, whereas the loss modulus is a

measure of fluidity, or the fluid's ability to dissipate energy. For a Newtonian fluid,  $G'=0$  (no elasticity), while for a perfectly elastic solid adhering to Hooke's law,  $G''=0$ .

To minimize the effect of particle sedimentation, all samples were subjected to a pre-shearing at 1500 s<sup>-1</sup> for 200 – 300 s followed by an equilibration time of 300 – 600 s. These values were selected after subjecting samples to a variety of pre-shearing and equilibration conditions and obtaining reproducible data.

## RESULTS AND DISCUSSION

### Oscillatory Shear Flow

We begin by probing the state of these exfoliated clay dispersions using oscillatory shear. Figure 3 shows data for the storage and loss moduli for 0.5 wt%, 1 wt%, 3 wt%, and 4 wt% C15A as well as 1 wt% EC15A as a function of the amplitude of the applied stress. The frequency of oscillation is fixed at an intermediate value of 1 rad/s, and the samples were allowed up to 600 s to reach equilibrium for reasons that will be discussed momentarily. At low stress amplitude, the samples show a plateau in both moduli, a solid-like response that is indicative of a networked, gel-like material. Also consistent with that observation, the plateau value of the storage modulus is an order of magnitude larger than that of the loss modulus in all cases.

Also, the storage modulus drops precipitously for all but the 0.5 wt% C15A sample at a particular value of the stress amplitude that increases with increasing clay loading. At this same time, the loss modulus also drops abruptly after a short period of increase. The abrupt drop in both moduli suggests a sudden transition from solid-like to liquid-like behavior, which is characteristic of yielding. In fact, the stress amplitude at which the storage modulus plummets is a reasonable estimate of the yield stress for each material. Accordingly, the yield stress increases with clay loading as one would expect if increasing clay content led to a more highly networked fluid. Finally, the fact that the 0.5 wt% sample has a more gradual transition from solid- to liquid-like behavior perhaps indicates a less structured clay network relative to the samples with higher clay loading.

The effect of removing excess surfactant is evidenced in the results for the 1 wt% EC15A solution in Figure 3. The

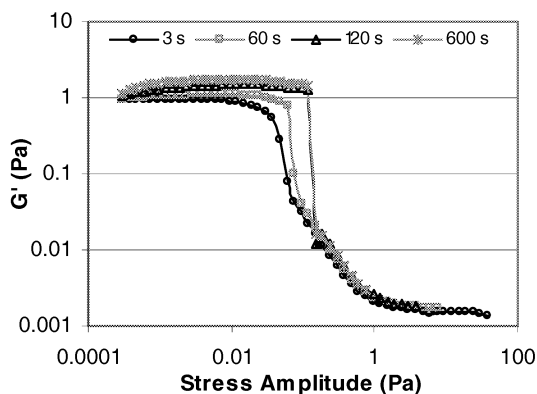


**Figure 4.** Storage modulus versus stress amplitude for the 1 wt% C15A solution with data acquisition times of 3, 60, 120, and 600 s. The frequency of oscillation is 1 rad/s.

moduli plateau values are similar to those of the 3 wt% C15A solutions, indicating that the excess surfactant plays a prominent role in reducing elasticity, perhaps by disrupting the network structure. Further experiments with the extracted clay at higher loadings are currently underway. Table 1 summarizes the yield stresses estimated from Figure 3.

As was mentioned previously, the results in Figure 3 were obtained by allowing up to 600 s for the samples to reach equilibrium at each value of the stress amplitude. To justify this choice of data acquisition time, we report storage modulus data for the 1 wt% C15A solution as a function of stress amplitude with data acquisition times of 3, 60, 120, and 600 s in Figure 4. Not only does the drop in storage modulus become sharper but the yield stress also shifts to higher values of the stress amplitude as the data acquisition time increases, until the data become indistinguishable at 120 s and 600 s. These results suggest that, in the vicinity of the yield stress, the networked structure is perturbed but stabilizes if given a sufficiently long equilibration time. The correlation of that time scale with clay loading and the physics of network stabilization remain unknown.

**Table 1.** Estimates of yield stress from oscillatory shear (Figure 3) and steady shear (Figure 5).

Sample	Yield Stress in Oscillatory Shear (Pa)	Yield Stress in Steady Shear (Pa)
0.5 wt% C15A	0.015	0.0075
1 wt% C15A	0.12	0.12
3 wt% C15A	0.24	0.24
4 wt% C15A	0.95	0.95
1 wt% EC15A	0.19	0.20

### Steady Shear Flow

Steady (or continuous) shear flow offers an alternative means by which the yielding behavior of fluids may be

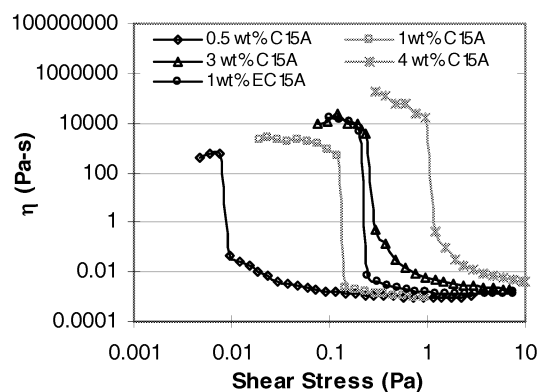


**Figure 5.** Viscosity versus shear stress in steady shear flow with shear stress ramping from low to high values.

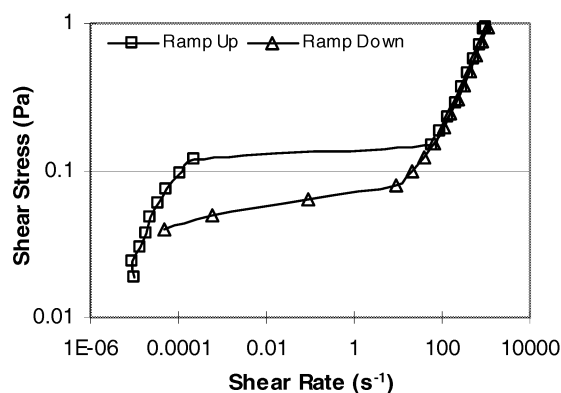


**Figure 6.** Shear stress versus shear rate hysteresis plot for 1 wt% C15A solution.

probed by plotting the viscosity versus shear stress. As with the oscillatory shear flows, each point was allowed up to 600 s to reach a steady state value. Referring to Figure 5, the steady shear data for viscosity bear a striking resemblance to the oscillatory shear data for the storage modulus. In each case, there is a high viscosity plateau at low shear stresses, where the fluid exhibits a solid-like response. The low shear stress viscosity increases significantly with clay loading, as the modulus did in oscillatory shear. After exceeding a critical shear stress (i.e., yield stress), the samples begin to flow, and the viscosity drops by up to 6 orders of magnitude. Presumably, the onset of flow marks the destruction of the clay network.

The sharp drop in storage modulus in Figure 3 and viscosity in Figure 5 gives two means by which the yield stress may be estimated for these solutions. These estimates may be found in Table 1. With the exception of the 0.5 wt% C15A sample, where yield behavior was less distinct in oscillatory shear, the yield stress estimates agree with one another.

One important question is whether the viscosity versus shear stress results are reversible. For instance, the data in Figure 5 were obtained by ramping the shear stress from low to high values. To determine if the network structure would reform at the yield stress or exhibit hysteric

**Table 2.** Estimates of shear stress versus shear rate hysteresis regions for all solutions based on results like those presented in Figure 6.

Sample	Stress Stress Hysteresis Range (Pa)	Magnitude of Shear Stress Hysteresis (Pa)
0.5 wt% C15A	0.0038 – 0.0075	0.0038
1 wt% C15A	0.040 – 0.15	0.11
3 wt% C15A	0.06 – 0.25	0.19
4 wt% C15A	0.50 – 1.26	0.76
1 wt% EC15A	0.08 – 0.25	0.17

behavior, we performed identical steady shear flow experiments in which the shear stress was ramped from high to low values. The customary for examining such data is to plot shear stress versus shear rate, as has been done in Figure 6 for the 1 wt% C15A solution. Here, we observe the classic hysteresis behavior of yield stress fluids. Once the yield stress has been exceeded, the network structure of the clay is unable to reform until the shear stress is reduced to a value significantly below the yield stress. In other words, once the network has been disrupted, flow can more readily prevent the network from reforming; hence, we observe the hysteretic loop of Figure 6. All the samples studied display similar hysteretic behavior, although the hysteresis region spans a larger range of shear stresses with increasing clay loading, as shown in Table 2. Additionally, the 1 wt% EC15A solution shows behavior similar to the 3 wt% C15A solution, again highlighting the role excess surfactant plays in disrupting the clay network.

The observed hysteretic behavior in the shear stress invites a deeper investigation into the time-dependence of the network structure near the yield stress. To that end, we present the viscosity as a function of time for the 3 wt% C15A solution for shear stresses of 0.25 and 0.3 Pa in Figure 7. We observe small amplitude periodic behavior in the viscosity developing approximately 30 minutes into the experiments. At higher shear stresses, the periodic response vanishes, and the viscosity becomes constant over long times. While a detailed understanding of the physics driving this phenomenon is still under investigation, one might speculate that it stems from the unstable balance between network formation and flow disruption in this shear stress regime. Additional experimental results will be forthcoming.

### Double-Step Shear Stress

Another point of interest is the time scale required for the clay network to reform after yielding. For instance, does the network reformation time depend upon clay loading or initial deformation? To address these questions, we performed so-called double-step shear stress experiments. The fluid is subjected to a constant shear stress (above the yield stress) until a steady state is achieved, after which the

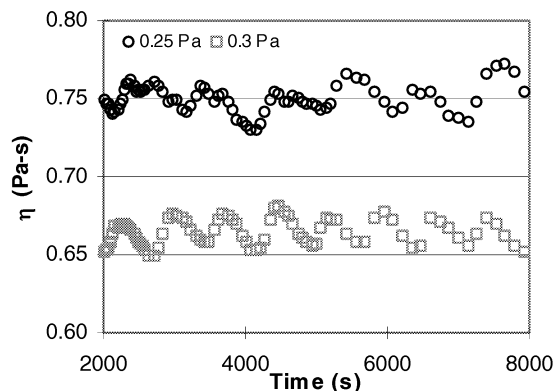


**Figure 7.** Viscosity versus time for 3 wt% C15A solution at shear stresses of 0.25 and 0.3 Pa, which are near the estimated yield stress for that sample.

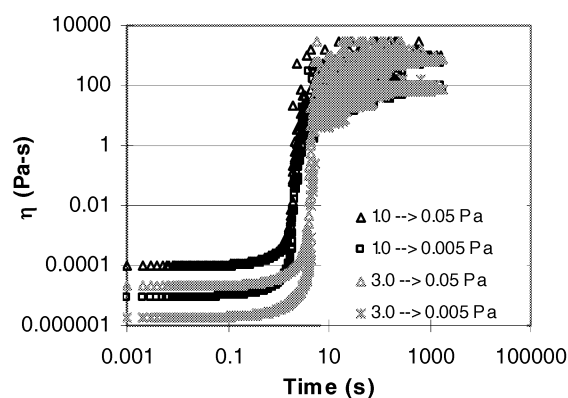


**Figure 8.** Viscosity versus time for 1 wt% EC15A solution in double-step shear stress experiments.

shear stress is abruptly reduced to a level below the yield stress and the time dependent viscosity is measured.

Figure 8 shows the results of four such double-step shear stress experiments for the 1 wt% EC15A solution. Two of the cases have initial shear stress of 3.0 Pa and final shear stresses of 0.05 and 0.005 Pa. The other two cases correspond to an initial shear stress of 1.0 Pa and the same final shear stresses. Although these preliminary data are somewhat flawed in that the experiments for the same initial shear stress do not have the same viscosity at time 0, the time at which the shear stress changes. Nevertheless, the qualitative results are likely valid. The most notable feature is that the time scale for network reformation appears to depend strongly on the initial shear stress rather than the final shear stress, in that the jump in viscosity occurs at the same time for the data with the same initial shear stress. From these results, one might infer that, even though the equilibrium clay network has been destroyed, the flow may orient individual clay platelets to a degree that depends upon the magnitude of the imposed stress. Following a reduction in shear stress, entropically-driven diffusion causes the clay platelets to begin disordering as part of the network reformation; however, the more highly

oriented platelets require a longer time to diffuse back to a networked state. Additional experiments are currently seeking to explore this hypothesis.

## CONCLUSIONS

We have reported mechanical rheological data for organically modified clay dispersions in p-xylene for clay loadings ranging from 0.5 wt% to 4 wt%. Samples have been subjected to oscillatory shear flow, steady shear flow, and double-step shear stress flows. All samples exhibit a solid-like response at low deformations in both oscillatory and steady shear, suggesting the existence of a percolated clay network. Oscillatory shear and steady shear both showed evidence of a yield stress whose value increased as the clay loading increased. The yield stress was also observed to increase when excess surfactant is removed from the solution. The yield stresses estimated in oscillatory and steady shear were effectively the same.

When the time-dependent response in the vicinity of the yield stress was examined, the viscosity exhibited a time-periodic response, suggesting that the balance between the tendency of the clay to form a network and the flow to disrupt that network are closely balanced. Consistent with this hypothesis, the periodic behavior vanished at shear stresses beyond the yield stress, where one would expect that flow would dominate.

Finally, double-step shear stress experiments were conducted to explore the time scale for clay network reformation. Samples were subjected to a constant shear stress above the yield stress until steady state was achieved, after which the shear stress was dropped to a level well below the yield stress. Though additional work is necessary, the preliminary data indicate that the initial shear stress controls the time scale for network reformation. We postulate that flow-induced platelet orientation may be responsible.

## REFERENCES

Hanley, H. J. M., C. D. Muzny, D. L. Ho and C. J. Glinka, "A small-angle neutron scattering study of a commercial organoclay dispersion," *Langmuir* **19**, 5575-5580 (2003).

Hanley, H. J. M., C. D. Muzny, D. L. Ho, C. J. Glinka and E. Manias, "A study of organoclay dispersions," *Int. J. Thermophys.* **22**, 1435-1448 (2001).

Ho, D. L., R. M. Briber and C. J. Glinka, "Characterization of organically modified clays using scattering and microscopy techniques," *Chem. Mat.* **13**, 1923-1931 (2001).

Ho, D. L. and C. J. Glinka, "Effects of solvent solubility parameters on organoclay dispersions," *Chem. Mat.* **15**, 1309-1312 (2003).

Kojima, Y., A. Usuki, M. Kawasumi, A. Okada, Y. Fukushima, T. Kurauchi and O. Kamigaito, "Mechanical properties of nylon 6-clay hybrid," *J. Mat. Res.* **8**, 1185-1189 (1993).

Vaia, R. A., W. D. Liu and H. Koerner, "Analysis of small-angle scattering of suspensions of organically modified montmorillonite: Implications to phase behavior of polymer nanocomposites," *J. Polym. Sci. Pt. B-Polym. Phys.* **41**, 3214-3236 (2003).

Zhong, Y. and S. Q. Wang, "Exfoliation and yield behavior in nanodispersions of organically modified montmorillonite clay," *J. Rheol.* **47**, 483-495 (2003).